International Tables for Crystallography (2012). Vol. F, Section 8.1.2, pp. 189–190.

PART 8. SYNCHROTRON CRYSTALLOGRAPHY

Chapter 8.1. Synchrotron-radiation instrumentation, methods and scientific utilization

J. R. Helliwell

8.1.1. Introduction

Synchrotron radiation (SR) has had a profound impact on the field of protein crystallography. The properties of high spectral brightness and tunability have enabled higher-resolution structure determinations, multiple-wavelength anomalous-dispersion (MAD) techniques, studies of much larger molecular weight structures, the use of small crystals and dynamical time-resolved structural studies. The use of SR required development of suitable X-ray beamline optics for focusing and monochromatization of the beam, which had to be stable in position and spectral character, for rotating-crystal data collection. Finely focused polychromatic beams have been used for ultra-fast data collection with the most advanced SR sources, where a single bunch pulse of X-rays can be strong enough to yield Laue diffraction data. The optimal recording of the diffraction patterns has necessitated the development of improved area detectors, along with associated data-acquisition hardware and data-processing algorithms. Sample cooling and freezing have reduced and greatly diminished, although not eliminated, radiation damage, respectively. In turn, even smaller crystals have been used. However, new X-radiation damage challenges are being reached. The low emittance of SR sources, with their small source size and beam divergence, corresponds well with the small size and low mosaicity of protein crystal samples. The evolution of SR source spectral brightness each year over the last twenty years has changed by many orders of magnitude, a remarkable trend in technical capability.

8.1.2. The physics of SR

The physics of the SR source spectral emission was predicted by Iwanenko & Pomeranchuk (1944) and Blewett (1946), and was fully described by Schwinger (1949). It is 'universal' to all machines of this type, *i.e.*, wherever charged particles such as electrons (or positrons) travel in a curved orbit under the influence of a magnetic field, and are therefore subject to centripetal acceleration. At a speed very near the speed of light, the relativistic particle emission is concentrated into a tight, forward radiation cone angle. There is a continuum of Doppler-shifted frequencies from the orbital frequency up to a cutoff. The radiation is also essentially plane-polarized in the orbit plane. However, in high-energy physics machines, the beam used in target or colliding-beam experiments would be somewhat unstable; thus, while pioneering experiments ensued through the 1970s, a considerable appetite was stimulated for machines dedicated to SR with stable source position, for fine focusing onto small samples such as crystals and single fibres, and with a long beam lifetime for more challenging data collection. Crystallography has been both an instigator and major beneficiary of these developments through the 1970s and 1980s onwards. An example of a machine lattice (the ESRF) is shown in Fig. 8.1.2.1.

The properties of synchrotron radiation can be described in terms of the well defined quantities of high flux (a large number of photons), high angular brightness (also well collimated), high spectral brightness (also a small source size and well collimated), tunable, polarized, defined time structure (fine time resolution) and exactly calculable spectra. The precise definition of the spectral brightness is

$$\text{Spectral brightness} = \text{photons per s per mm}^2 \text{ per mrad}^2 \text{ per (0.1\% bandwidth)}. \qquad (8.1.2.1)$$

Care needs to be exercised to check precisely the definition in use (Mills *et al.*, 2005). The mrad^2 term refers to the radiation solid angle delivered from the source, and the mm^2 term to the source cross-sectional area. Mills *et al.* (2005) concluded that the units given in equation (8.1.2.1), which do not follow the SI code for

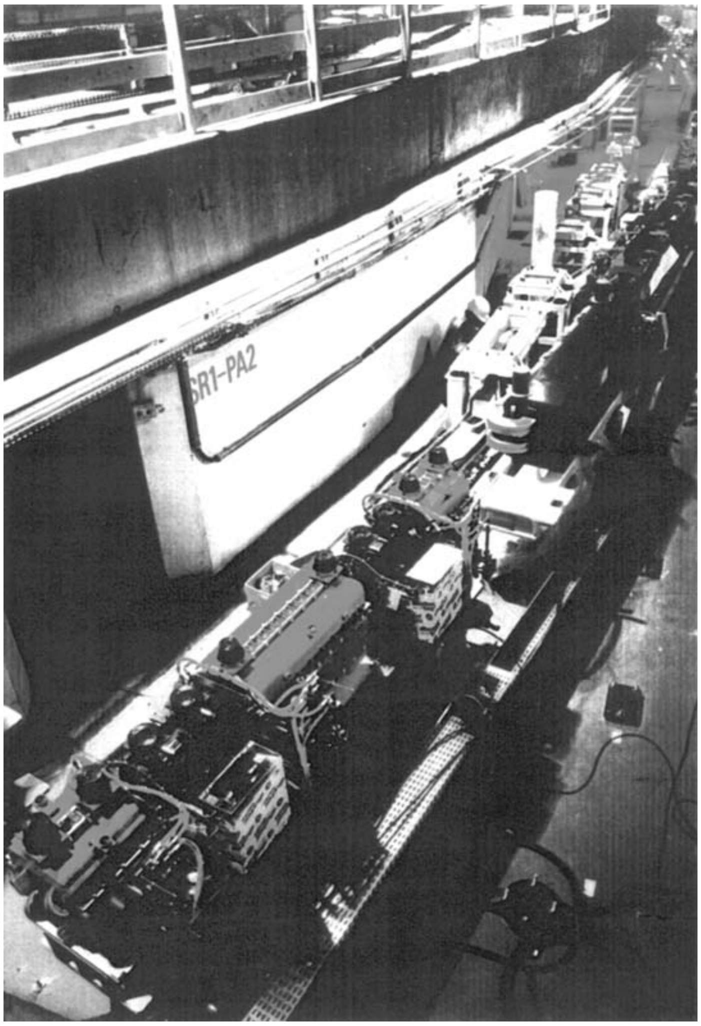

Figure 8.1.2.1
The ring tunnel and part of the machine lattice at the ESRF, Grenoble, France.

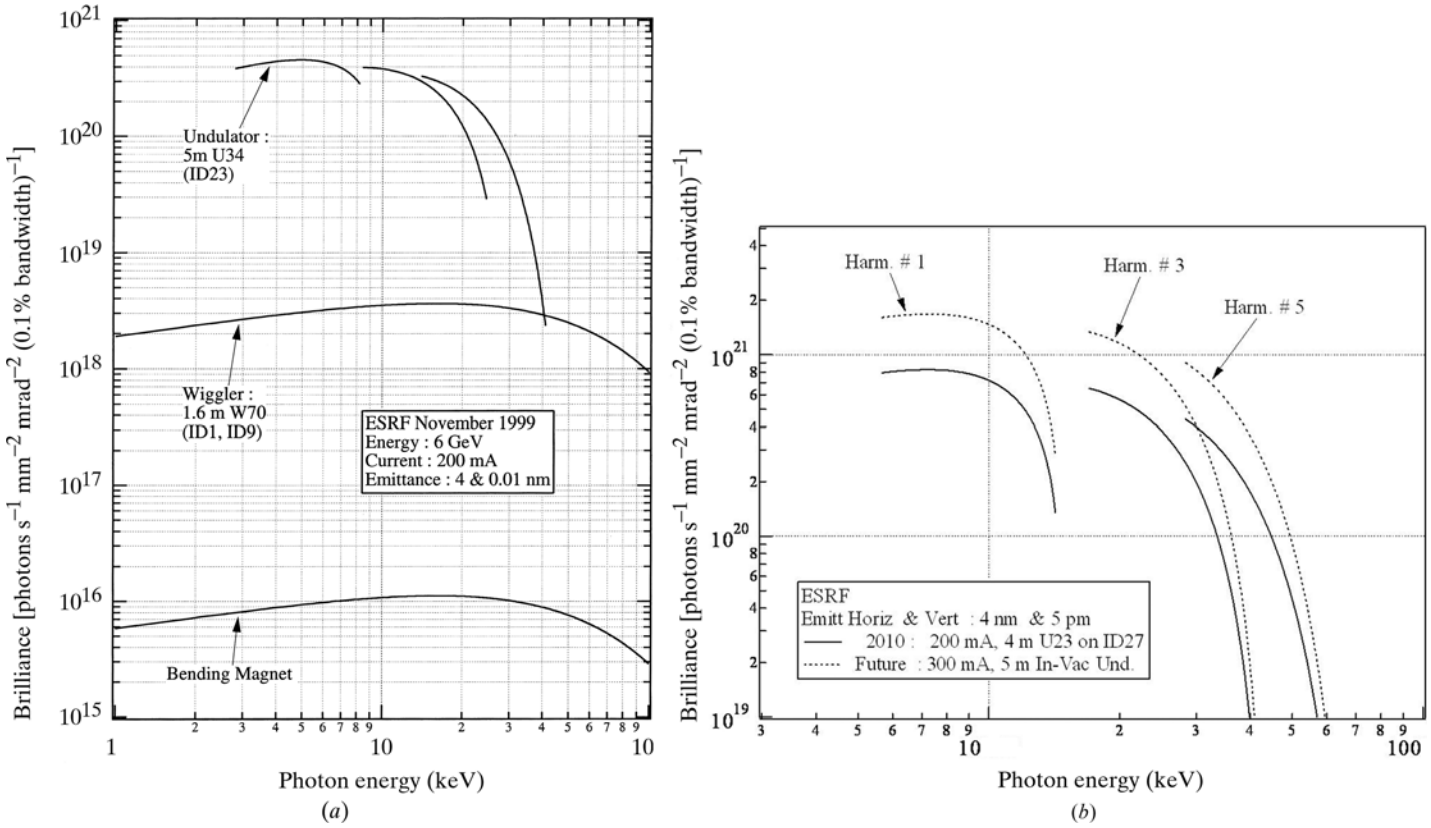

Figure 8.1.2.2

SR spectra. (*a*) Spectral brightness (also referred to as brilliance) of different SR source types (undulator, multipole wiggler and bending magnet) as exemplified by such types of sources at the ESRF. For the undulator, the tuning range (*i.e.* as the magnet gap is changed) is indicated. (*b*) Brilliance produced by the in-vacuum undulator of cell 27 of the ESRF dedicated to high-pressure studies. The plain curve corresponds to the condition in use as of September 2010. Further increase in brilliance (dotted curve) is expected in the years to come by increasing the ring current, increasing the length of the undulator and further decreasing the vertical emittance. Kindly provided by Dr Pascal Elleaume, ESRF, Grenoble, France.

units, are so ensconced in the field 'that a drive to change this would only lead to more confusion rather than more clarity in the descriptions of synchrotron-radiation sources'. At the ESRF the term brilliance is firmly ensconced in house and with its large user community, and so is the label for the *y* axes used in Fig 8.1.2.2.

Another useful term is the machine emittance, ε. This is an invariant for a given machine lattice and electron/positron machine energy. It is the product of the divergence angle, σ', and the source size, σ:

$$\varepsilon = \sigma\sigma'. \qquad (8.1.2.2)$$

The horizontal and vertical emittances need to be considered separately.

The total radiated power, Q (kW), is expressed in terms of the machine energy, E (GeV), the radius of curvature of the orbiting electron/positron beam, ρ (m), and the circulating current, I (A), as

$$Q = 88.47E^4I/\rho. \qquad (8.1.2.3)$$

The opening half-angle of the synchrotron radiation is $1/\gamma$ and is determined by the electron rest energy, mc^2, and the machine energy, E:

$$\gamma^{-1} = mc^2/E. \qquad (8.1.2.4)$$

The basic spectral distribution is characterized by the universal curve of synchrotron radiation, which is the number of photons per s per A per GeV per horizontal opening in mrad per 1% $\delta\lambda/\lambda$ integrated over the vertical opening angle, plotted versus λ/λ_c. Here the critical wavelength, λ_c (Å), is given by

$$\lambda_c = 5.59\rho/E^3, \qquad (8.1.2.5)$$

again with ρ in m and E in GeV. Examples of SR spectral curves are shown in Fig. 8.1.2.2(*a*). The peak photon flux occurs close to λ_c, the useful flux extends to about $\lambda_c/10$, and exactly half of the total power radiated is above the critical wavelength and half is below this value.

In the plane of the orbit, the beam is essentially 100% plane polarized. This is what one would expect if the electron orbit was visualized edge-on. Away from the plane of the orbit there is a significant (several per cent) perpendicular component of polarization. Schiltz & Bricogne (2009) advocated definitions to use in the analysis of polarization-dependent phenomena that are instrument-independent and completely general. They have implemented these methods in the macromolecular phasing program *SHARP* for exploiting the polarization anisotropy of anomalous scattering in protein crystals.

8.1.3. Insertion devices (IDs)

These are multipole magnet devices placed (inserted) in straight sections of the synchrotron or storage ring. They can be designed to enhance specific characteristics of the SR, namely

(1) to extend the spectral range to shorter wavelengths (wavelength shifter);
(2) to increase the available intensity (multipole wiggler);
(3) to increase the spectral brightness *via* interference and also yield a quasi-monochromatic beam (undulator) (Fig. 8.1.2.2*b* shows the distinctly different emission from an undulator);

references